Front. Chem. Sci. Eng. 2019, 13(3): 427–443
https://doi.org/10.1007/s11705-019-1805-4

REVIEW ARTICLE

Tailoring electrical conductivity of two dimensional nanomaterials using plasma for edge electronics: A mini review

Aswathy Vasudevan[1,2], Vasyl Shvalya[1], Aleksander Zidanšek[1,2,3], Uroš Cvelbar (✉)[1,2]

1 Jožef Stefan Institute, 1000 Ljubljana, Slovenia
2 Jožef Stefan International Postgraduate School, 1000 Ljubljana, Slovenia
3 Faculty of Natural Sciences and Mathematics, University of Maribor, 2000 Maribor, Slovenia

Abstract Since graphene has been discovered, two-dimensional nanomaterials have attracted attention due to their promising tunable electronic properties. The possibility of tailoring electrical conductivity at the atomic level allows creating new prospective 2D structures for energy harvesting and sensing-related applications. In this respect, one of the most successful way to manipulate the physical properties of the aforementioned materials is related to the surface modification techniques employing plasma. Moreover, plasma-gaseous chemical treatment can provide a controlled change in the bandgap, increase sensitivity and significantly improve the structural stability of material to the environment as well. This review deals with recent advances in the modification of 2D carbon nanostructures for novel 'edge' electronics using plasma technology and processes.

Keywords graphene, edge electronics, 2D nanomaterials, plasma, electrical conductivity

1 Introduction

Nanomaterials for electrochemical applications include the one-dimensional (1D) structures like nanoribbons, nanotubes and nanowires, the two-dimensional (2D) including single atom thick nanomaterials, nanowalls, nanoflakes and the three-dimensional (3D) such as quantum dots, nanoparticles, nanoballs and nanocones [1]. At various dimensions, the same chemical composition and structure can exhibit different properties while considering reduced scales. Graphene is an excellent material that can demonstrate this scaling effect. For example, below 10 nanometers, bandgap and transport properties are being changed, which is directly reflected in electrical conductivity. In 2005, Novoselov and co-workers presented graphene as a dense honeycomb crystal structure that can be considered as unrolled single-wall carbon nanotubes (SWCNTs). The authors have shown that the conductivity of one layer graphene sheet cannot be lower than a minimum value corresponding to the quantum unit of conductance, even when charge carriers concentrations approach to zero. Moreover, graphene possesses a strong integer quantum Hall effect at half-integer filling factors [2].

After discovering 3-dimensional fullerene and 1-dimensional carbon nanotubes (CNT), the carbon-based nanostructures became the most frequently studied nanomaterials. Most of the synthesised new low-dimensional structures, such as nanoribbons obtained from 2D crystals [3–5], revealed characteristic sp^2-hybridised chemical bonds. This type of hybridisation can also be found in other non-carbon contained 2D materials. By affecting sp^2-hybridised bonds with different tools, such as plasma, the electrical conductivity, capacitance and catalytic properties of these materials can be altered in a controlled way.

Due to their promising electronic properties, the majority of all 2D materials can be classified into several groups: 2D semiconductors, 2D ferromagnetic, 2D superconductors, 2D semimetals, 2D topological insulators, 2D metals. The mother of all those perspective materials is graphene, which in turn, opened the path for synthesising low-dimensional structures such as transition metal dichalcogenides (TMDs), transition metal oxides (TMOs), transition metal hydroxides (TMHs), elemental 2D phosphorene, germanene, tinene and silicene. In recent years, single layered TMDs are becoming increasingly important due to their

Received September 29, 2018; accepted December 6, 2018

E-mail: uros.cvelbar@ijs.si

diverse electrical properties and natural abundance. For TMDs a generalised chemical formula MX_2 is used, wherein, 'M' typically represents a transition metal of the groups 4–10 (Mo, Nb, W, Ni, V, or Re) [8], where X is a chalcogen (Se, Te, or S) [9–11]. TMDs possess very diverse electronic structures, ranging from superconductors ($TaSe_2$, $NbSe_2$) to insulators (HfS_2), making them versatile for electrochemical energy storage applications [12]. Later, semiconducting molybdenum disulfide (MoS_2) got the attraction of researchers for energy storage applications [13] by functionalisation and defect engineering of this 2D TMDC material. Semimetals like $TiSe_2$, and metals like $NbSe_2$, are known because they exhibit superconductivity behaviour at low temperature [14–16]. Correspondingly, the newly developed 2D nanosheets of transition metal dichalcogenides and metal oxides with interesting electronic structure are being comprehensively investigated [17]. Similarly, TMOs have promising optical properties due to their characteristic bandgap. For example, MnO_2 has a bandgap of 2.1 eV and exhibits a strong photoelectrochemical response to visible light [18]. Silicenes and phosphorenes are elemental semiconducting materials that possess an inherent direct bandgap and exhibit similar electrical properties as graphene [15,16]. The bandgap of graphene and its analogues from this group (silicene, germanene, and tinene) increases along the row C → Si → Ge → Sn. Currently, known members of the 2D material family are listed in Table 1 [19]. For real practical applications, the structural stability of these materials plays a crucial role. Monolayers of graphene, 2D chalcogenides, semiconducting dichalcogenides ($MoTe_2$, WTe_2), and 2D oxides (MnO_2) are stable under ambient environments. However, the metallic dichalcogenides ($NbSe_2$, NbS_2) and layered semiconducting chalcogenides (GaSe, GaTe) are stable only in inert atmospheres [17].

Prospective electronic transport properties [20], mechanical stability [21], photoelectrochemical response [22], and temperature dependence of the bandgap [23] make these materials suitable for applications in electronic devices, sensors, catalysts, energy harvesting, and data storage devices [12].

2 Electronic properties of graphene

The 2D materials possess unique properties due to their structural characteristics and quantum size effects associated with their layer thickness [24]. Nano-sized thin layers can allow a close contact between the interfacial layers. Notable variations in the physical and chemical properties are also observed in such layered materials due to the electron confinement effect. However, the absence of interlayer interaction is significant when we explore their band structure. Those one-atom-thick layers enable direct access and simple processing of the mobile charge carriers and their high carrier mobility even at low temperatures [25]. Since the manuscript is mostly related to the electrical properties of 2D materials and possible routes of their modifications, a brief description of graphene band structure is presented in this section.

The unit cell of graphene includes two carbon atoms which are gathered in a well-known hexagonal honeycomb structure (Fig. 1(a)) [26]. The electronic structure consists of valence and conduction bands formed by π- and π* states, respectively. The band diagram is characterised by six highly symmetric K and K' points, known as Dirac points E_{Dirac}, where the energy distance between two zones is close to zero (Fig. 1(b)). In the low energy region, which is important for electron transport, dispersion reveals a linear behaviour (Fig.1(c)). As a consequence, the characteristic band structure can be considered as two cones in touch at E_{Dirac} (Fig. 1(d)). Since both valence and conduction bands in graphene are in touch, new energy states form near the Fermi levels (see Fig. 1(d)), which are sensitive to external influences, such as electric fields, plasma interactions, mechanical deformations, doping and adsorption. This property is very desirable in sensing applications, making graphene-based materials suitable for electrochemical energy storage [27–29]. Outstanding electrical properties of graphene are caused by the linear dispersion relation of charge carriers, which mimic massless relativistic particles [2]. The transport properties of graphene are also attributed to the absence of long-range interaction backscattering processes. As a result, the electron/hole elastic mean free path is about hundreds of nanometers. In graphene, additional scattering mechanisms take place, which is initiated by acoustic and optic phonons. In the acoustic case, the scattering is rather weak, while for the optic waves it becomes relevant only at very high frequencies (~1600 cm^{-1} or ~4.8×10^{13} Hz). The last case is outside the scope of our study, as we do not deal with the high electric field. The elastic and inelastic collisions are the subject of interest in long graphene

Table 1 An overview of 2D materials according to their electrical conductivity properties

2D material	Members	Examples	Ref.
Conductors	2D metals, carbon-based materials	BiTe, BSCCO, FeTe, NbS_2,VSe_2, graphene	[6]
Semiconductors	2D metal chalcogenides, 2D halides, 2D phosphides, 2D arsenide, 2D oxides, elemental	Tellurene, black phosphorus, CuS, SnS, MoS_2, WS_2, $SnSe_2$, BPS, $FePS_3$, $FePSe_3$, $As2S_3$, As_2Se_3, MnO_2, PbI_2, CdI_2	[7]
Insulators	*h*-BN, 2D hydroxides, 2D micas	MoO_3, Sb_2OS_2, $Ca(OH)_2$, $Mg(OH)_2$	[7]

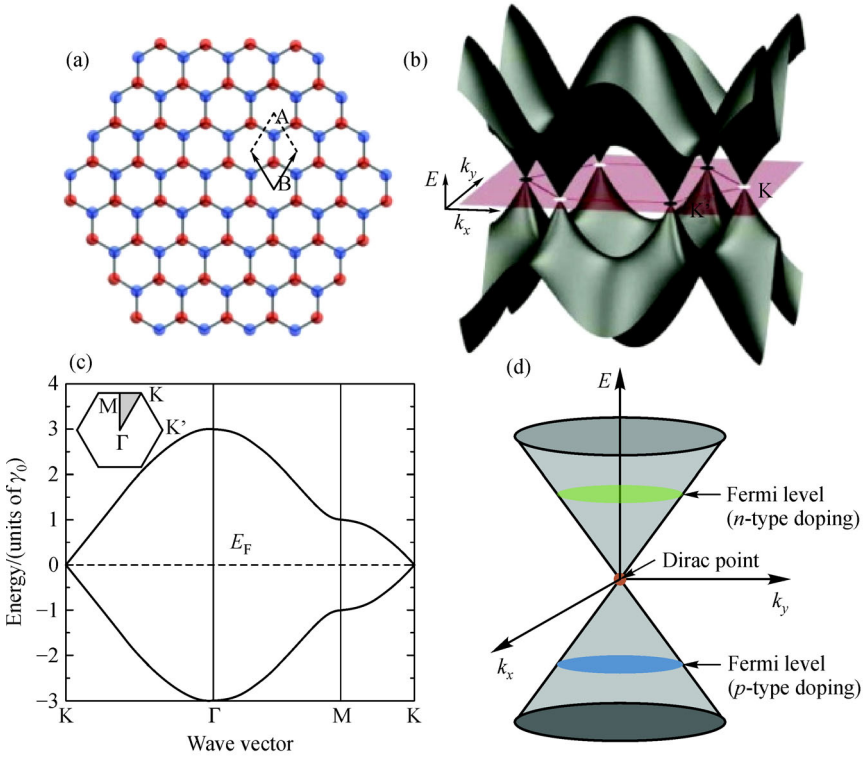

Fig. 1 Electronic structure of one layer graphene. (a) Honeycomb lattice structure of graphene consisting of two atoms (A and B); (b) The representation of the graphene band structure; (c) Phonon spectra of graphene. (d) The schematic representation of low energy band structure exhibiting zero energy gap at the Dirac point. 'Blue' and 'green' Fermi levels reveal *p*- and *n*-dopants states (reprinted with permission from the reference [26])

channels or in 2D nanostructures like nanoribbons, where the transport is changed from ballistic to diffusive [26]. In the case of 2D carbon nanostructures the scattering processes are mainly produced by impurities, defects or/and short-range phonon-phonon interactions, thus drastically reducing the mean-free path. In fact, the elastic collisions mechanisms caused by charged impurities, adsorbents and edge roughness are usually referred to as Coulomb scattering. On the other hand, the inelastic collisions that arise due to the acoustic and optical phonons can also contain the surface phonons of an insulating substrate [30]. Moreover, the scattering mechanisms and transport properties also depend on the edge structures and morphologies.

3 2D carbon nanostructure morphologies and transport properties

Two-dimensional structures can also be classified based on their interlayer bonding forces: layered van der Waals solids, layered ionic solids, and surface assisted non-layered solids. Layered van der Waals solids exhibit strong covalent or ionic bonds within the plane and weak van der Waals or hydrogen bonding out of the plane. They include atomically flat graphene, boron nitride (*h*-BN), phosphorene, transition metal dichalcogenides (TMDs), layered metal oxides. Layered ionic solids are 2D materials, which are assembled form of a charged polyhedral layer sandwiched between hydroxide or halide layers coupled by electrostatic forces. Compounds such as $La_{0.90}Eu_{0.05}Nb_3O_{10}$, $KLnNb_2O_7$, $Eu(OH)_{2.5}(DS)_{0.5}$ belong to this group. Surface-assisted nonlayered solids are materials comprised of an atomically thin-layered material, typically synthesised on a substrate via chemical vapour deposition (CVD) and epitaxial growth. Silicene and germanene are typical representatives of this category.

Interestingly, the deposition and growth of the 2D materials depend significantly on the medium and the substrate surface. During the epitaxial growth of structures on a substrate (usually a metal), the nanostructures like nanowalls, nanoislands and nanodisks are formed. These morphologies exhibit characteristic edges, which unveil different electronic structures compared with the centre areas of the islands [31]. Some characteristic two-dimensional shapes observed in literature are collected in Fig. 2. One of the most frequently obtained particles arrangements that grow on a substrate are nano-islands. The typical case of the gold island film prepared by vapour deposition [32] on top of the transparent substrates is

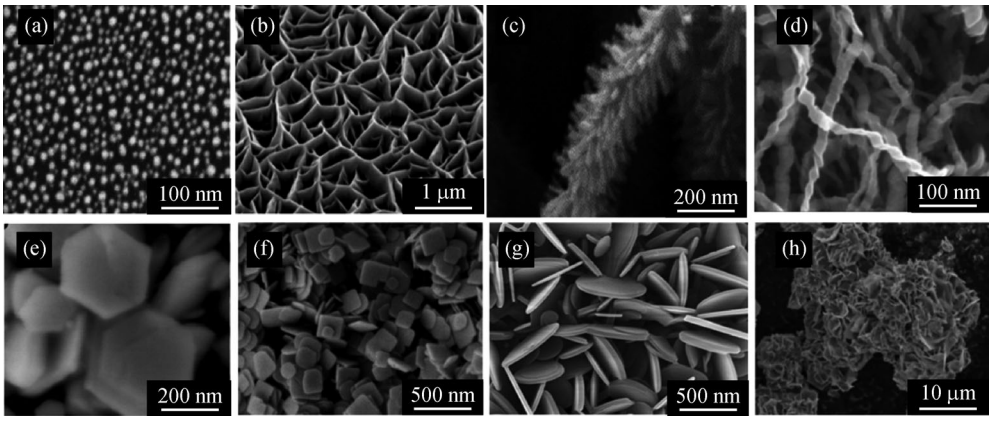

Fig. 2 Electron microscope images of different types of two-dimensional nanostructures. (a) Nano-island structure [37]; (b) Nanowalls [38]; (c) Branched nanostructures [39]; (d) Nanoribbons [40]; (e) Nanoplates [41]; (f) Nanodisks [42]; (g) Nanosheets [43]; (h) Nanoflowers [44]. (Reprinted with permission from the references listed above)

presented in Fig. 2(a). Nanodisks are the circular structures with specific enclosed edges. BiOCl single-crystal nanodisk (Fig. 2(e)) is for example used in photocatalytic activities due to its surface properties [33]. Branched nanostructures like for example ZnO branched nanowires are typically characterised by a higher surface area (Fig. 2(c)), which could be used in the photochemical cell for hydrogen evolution in water splitting [34]. Nanosheets and nanoplates are the flat 2D structures limited in surface area, which can be self-standing or bound to the surface. Examples are presented in Fig. 2(f) [35] and Fig. 3(g) [36].

2D nanosheets are materials with atomic or molecular thickness and large planar lengths so that the edges are not significant. The quantum confinement effects within the 2D layer govern the changes in electronic behaviour. The large surface-to-volume ratio and confined thickness to atomic scales offer incredibly high carrier mobility, the feasibility of chemical doping, mechanical flexibility, chemical stability, and optical transparency. This offers new potentials for the development of novel sensors and superior energy conversion and storage devices. Inspired by graphene, TMDs and TMOs have also been exfoliated and studied. Even though the excellent electrical conductivity of graphene makes it a transparent conductor, its zero bandgap limits its technological applications in electronic devices. However, TMDs (e.g., MoS_2) and TMOs (e.g., SnO) have a finite bandgap and therefore exhibit semiconducting behaviour. However, the exfoliation and the growth processes can make defects and impurities in 2D layers, which can alter their electronic properties. For example, in the SnO, exfoliated SnO monolayers the bandgap is wide as compared to layered structure because of the lack of electron lone pair interactions between the layers [45]. The defects form during the growth and can be tailored using adatoms like boron, carbon, nitrogen, oxygen, and fluorine, which can vary the number of valence electrons and therefore their transport properties.

Nanoribbons (NR) are flat 2D materials with a characteristic width of a few atoms, which are made up of a single or a few atoms thick lamellar crystals. Because of their narrow width edges are significant, and nanoribbons possess unusual optical and optoelectronic properties. We can vary these properties using different methods such as doping, selective functionalisation, applying external electrical/magnetic field or mechanical strain [46]. One of the widely used methods to obtain graphene nanoribbons is unzipping of CNT [47].

The characteristic width of NR is around 10 nanometers. Depending on the edge structure, non-chiral graphene nanoribbon (GNR) can be divided into two groups: armchair and zigzag. The principal difference in both shapes is defined by 30 degrees shift in their cutting direction. According to the classical nomenclature, the armchair shaped edges are characterised by the number of dimer lines (N_A) across the ribbons (Fig. 3(a)). On the other hand, the elemental pieces of the zigzag-like structure are zigzag chains (N_Z) (Fig. 3(b)) [48]. These two terminations make a clear difference between 2D graphene and NRs, simultaneously, giving rise to quantum confinement effect.

There have been only a few experimental studies on large 2D sheets and nanowalls, some of which are given in references [38,49,50]. It is difficult to investigate these materials because of their complicated synthesis and manipulation of the growth process. The main question is how to adapt their properties for implementation in the next generation nanoelectronics and also for advanced quantum computational devices. In the case of graphene, one approach to modifying its gapless nature is to transform them into narrow ribbons and thus obtain a finite energy gap. Graphene nanoribbons (GNRs) also show a local resonance within the energy gap. Because of

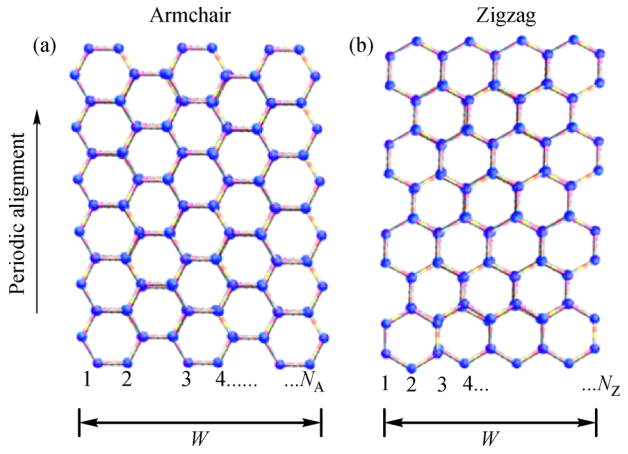

Fig. 3 Typical geometries of nanoribbons edges. (a) Armchair type arrangement: N_A is the number of dimers; (b) Zigzag type alignment: N_Z is the number of elements in the chains and W is the characteristic width [48]

that, the transport is carried out by the hopping of charge carriers through a quantum dot series [51]. A lot of theoretical studies were done on the transport mechanisms in GNRs. In nanoribbons, with width under a few nanometers, quantum confinement and edge effect are important and lead to exciting semiconducting features [52]. Earlier studies found that the armchair edged GNRs were typically semiconductors with gap size being inversely proportional to the ribbon width [53]. Quite the opposite happens with the zigzag edged GNRs (ZGNRs) in which metallic behaviour is linked to the localised edge states near the Fermi level. Later, the existence of a small bandgap in symmetric ZGNRs under bias voltage was also found by Li et al. [54]. Similar studies have been performed on phosphorene and bismuth nanoribbons [55,56]. The structure and chemical termination of the edges influence the charge carrier transport and thereby also device operation. The bonding characteristics between atoms change sharply at the edges, which can be used for functionalisation. Various nano-fabrication strategies including top-down and bottom-up strategies were adopted to realise nanoribbon structures in the sub-50 nm and even the sub-10 nm scale. From experimental observations of electrical properties like charge transport, edge disordered localisation and opening energy gaps can be explained as follows: (a) Transport behaviour due to intrinsic scattering, photon scattering, and impurity scattering. In general, the room temperature charge transport in nanoribbons is limited by intrinsic phonon scattering from the supporting substrate, impurity scattering, and edge roughness scattering [57,58]. It was reported that the carrier mobility starts to decrease when the ribbon width shrinks, because of the effect of the line edge roughness scattering [59,58]. Significantly smaller mobilities in chemically derived GNRs (200 $cm^2 \cdot V^{-1} \cdot s^{-1}$ with a ribbon width of 2 nm) [60] were observed due to rough edges. In the top-gated graphene-nanoribbon transistors made of 15-nm width GNRs etched with 50-nm ZrO_2 nanowires, the hole mobility was found to be of 1310 $cm^2 \cdot V^{-1} \cdot s^{-1}$, which is one of the highest values realised in GNR devices [61]. Until now, the influence of edge structure on the electronic properties of GNRs could only be verified with the study of the local density of states [62], which showed the existence of energy gaps for predominantly armchair-edged nanostructures. The width of the energy gaps decreases with increase in the ratio of zigzag versus armchair edges N_Z/N_A [63]. Figure 4 displays three possible ways of edge scattering: (1) Diffusive edge DE: the electrons are bouncing back and forth between the two edges, with a coefficient of the probability of being diffusely scattered P; (2) Structural edge-roughness SER: in this case, the ribbon edge structure is not uniform. Thus, the appropriate model, which describes the mobility degradation, has to be accompanied by width variations of the ribbons;

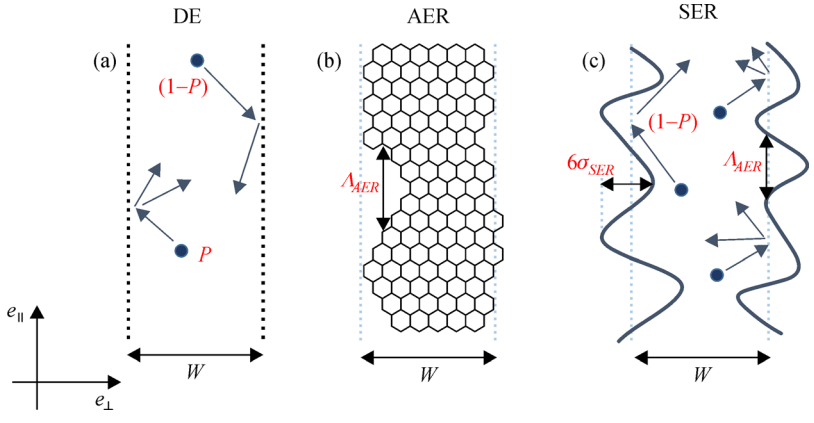

Fig. 4 Schematic representation of edge scattering mechanisms in graphene NRs. (a) DE-diffusive edge scattering; (b) Atomistic edge-roughness scattering; (c) Structural edge-roughness scattering. The coefficients are defined as follows: P is a probability collision coefficient, σ_{SER} is a standard width deviation, Λ_{SER} is SER correlation length, Λ_{AER} is AER correlation length, W is the characteristic width [64]

(3) Atomistic edge-roughness AER: the model is based on a modification of the nanoribbon edge by adding or subtracting one row of carbon atoms on each side [64]. (b) Edge roughness induced localisation effect. The transfer of electron wave function can be primarily hindered due to the quasi-one-dimensional Anderson localisations which are induced by edge disordering. That is, the suppression of conductivity near the charge neutrality point would occur with moderate edge roughness [65]. The calculation of the local density of states shows that the edge disorder can produce a strong enhancement of the electron density at the edge to form surface like localised states which do not participate in the charge transport [66]. The extracted localisation length depends on the disorder type. It decreases with the increase of disorder amplitude and with the reduction of ribbon width. Also, the localisation length reaches its minimum when the energy level approaches the Dirac point, resulting in enlarged transport gaps. A transport gap would develop where all the conducting channels were suppressed with the increasing disorder probability and ribbon length. The Anderson localisation induced transport bandgap was found not only in the edge-disordered armchair nanoribbons but also in the zigzag arranged NRs. The suppression of orientation effect was also predicted with the intensive disorder in which two rows of edge atoms were involved [67]. (c) Coulomb blockade effect. Another critical factor to be considered is the Coulomb blockade effect, which is due to the trapping of electrons on an island due to its charging effect under certain voltage conditions. It confirms the existence of a potential which is non-uniform, and it is associated with the quantum confinement of the carriers along the ribbon. This effect also prevents the Klein tunnelling processes [68] and creates a region of reduced conductivity inside. This effect was first observed in graphene quantum dot structure fabricated by e-beam lithography, in which a graphene island functioned as a quantum dot, while the bulk graphene served as electrodes and the graphene necks with a reduced width in between served as the tunnelling barriers [69,70]. Similar to this quantum dot structure formed by width tailoring, nanoribbons with large edge roughness may also undergo such dot-neck segregation. Therefore, they can be modelled as multiple graphene quantum dots in a series. Moreover, multiple Coulomb blockade effect was expected at low temperature. Sols and co-workers calculated the transport behaviour of edge disordered GNRs due to the Coulomb blockade effect [51]. Their result indicated that the Coulomb charging energy could open up an energy gap at low temperature.

The general idea of the Coulomb charge blocking effect in graphene nanoribbons is similar to the working principle of one electron transistor with two junctions. In the case of 2D NRs, the origin of reduction in conductance can be attributed to the localised charged defects (dots or necks) or the bandgap transformations [71]. Taking into account that the band structure is an inner property of the material, the energy gap rises due to electron-electron interaction and additionally supported by randomly localised charge carriers. In (Fig 5(a)) the typical trend of

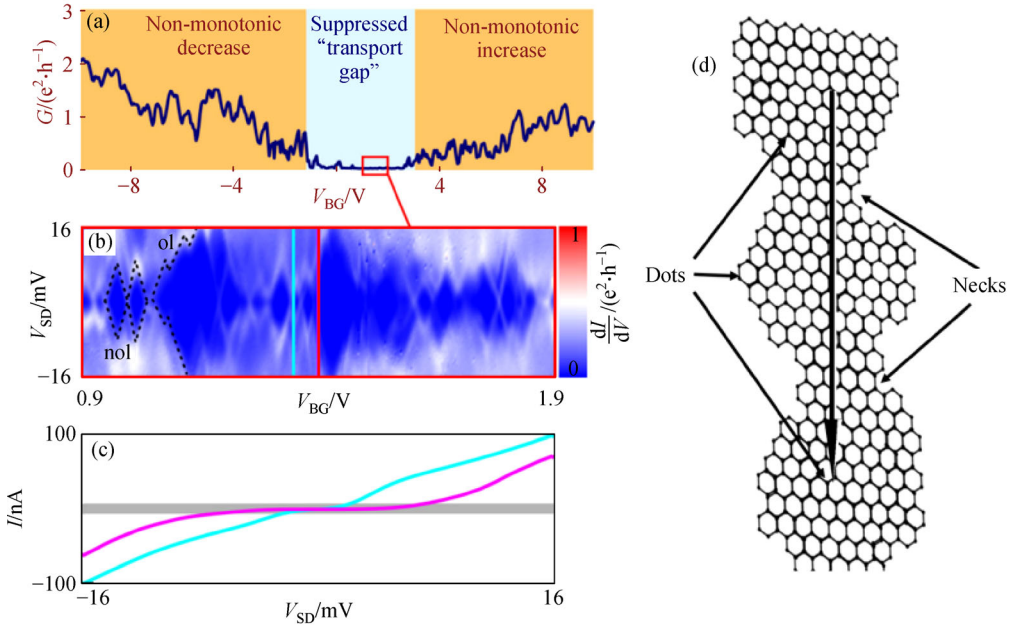

Fig. 5 Electric properties of graphene nanoribbons. (a) The low-temperature conductance of NR nanoribbons versus of applied gate voltage; (b) Conductance behaviour inside of the selected region; (c) Electrical current versus of applied bias voltage along two marked lines; (d) Dot-neck structure in disordered graphene nanoribbons. The disordered edge leading to the formation of dots and necks, where Coulomb-blockade takes place when the charge moves from one dot another [71]

the low-temperature conductance versus applied back voltage of graphene NRs is displayed. There are three different zones which can be considered. Those two regions coloured by orange represent a transition mode, where the electrons have higher energy than a certain barrier value that allows tunnelling through it. The middle grey region with suppressed current flow clearly demonstrates the Coulomb blockade effect. In this regime, the applied back gate voltage is too low. Thus, the energy of the electrons does not exceed the barrier value making impossible tunnelling processes. As a result, the conductance reaches its minimum. This effect can be visualised by plotting the differential conductance dI/dV_{SD}. The observed blue rhombuses are known as 'Coulomb diamonds' (Fig. 5(b)). Figure 5(c) presents the cross-section of the current flow as a function of applied bias voltage V_{SD} [71]. The Coulomb-blockade effect in nanoribbons is directly attributed to the roughness at the ribbon edges of the dot-neck structure as presented in Fig. 5(d). This roughness occurs naturally and leads to the charge localisation at the edges. Therefore, the formation of necks causes an abrupt reduction of the conducting channels and a significant increase in the impedance along the sheet. Due to this the conductance drastically drops to zero while approaching the charge-neutrality point even in the absence of a true bandgap. It ends up in the isolation of nanoscale size regions-dots. Inside this dot regions, the electrons are temporarily confined and Coulomb-blockade results from the electron transport in dot-to-dot through graphene necks.

The edge dominated carbon nanostructures can, therefore, possess a zero or non-zero bandgap, exhibiting metallic or semiconducting behaviour. Altering of a bandgap width allows creating new low dimensional materials with diverse electronic properties.

4 Tailoring of conductivity of two-dimensional materials

The demand for better electrical properties and simplification of nano-based devices requires the development of advanced 2D materials [72]. Tailoring these type of structures started by combining the building blocks and turning them into complex architectures [73]. To achieve the desired electrical, structural, optical and chemical properties, different approaches were used, like micromechanical exfoliation [21]. Most of these adjustments were successful in graphene and other 2D materials like MoS_2 [21,25]. The conductivity and transport properties are associated with the material bandgap, which should be introduced without compromising other properties. Various strategies of a bandgap opening in 2D materials like graphene are discussed below.

4.1 Quantum confinement in graphene nanoribbons

Graphene is a very suitable material for future nanoelectronics, which could replace even silicon and conductive interconnects. However, it is only useful after the bandgap is induced in its electronic structure. This bandgap can, for example, be effectively achieved by nanoribbon formation and quantum confinement of electrons. Unlike in a large area graphene, the electrons in quasi-one-dimensional nanoribbons (formed from 2D graphene sheets) are confined in a single dimension and make a finite bandgap semiconductor similar to carbon nanotubes. The theoretical model of nanoribbons was initially developed by Nakada et al. in their study of the edge effect. They proposed a possibility that the π electrons can exhibit a special electronic state near to the Fermi level, which would affect the electrical properties. They also demonstrated mathematically that carrier mobility and charge scattering are only expected at the edges [74]. In another work, Wakabayashi studied the electronic transport properties through nanographite ribbon junctions connecting two zigzag ribbons with same or different width by the Landauer-Buttiker approach using a tight-binding model. They found the conductivity is associated with a quasi-bound state in the scattering regions of the junctions, yielding the formation of standing waves [75]. They extended there work in the electronic states of graphite ribbons with edges of two typical shapes; armchair (Fig. 6) and zigzag, by performing tight binding band calculations. They found that the graphite ribbons exhibit the striking contrast in the electronic states depending on the edge shape [76]. Later, it was found that the graphene nanoribbons (GNRs) with a width greater than 10 nm have a finite bandgap as well as notable carrier mobility and thus high switching ratios [77]. Berger et al. demonstrated the nanoribbon geometry and electronic confinement along with coherence and Dirac nature of the carriers [78]. Ponomarenko et al. [69] also described the nanoribbons in quantum dot geometry. However, the semiconducting properties of GNRs below 10 nm would reduce the limitations of the SWCNTs due to their chirality dependence. Moreover, metallic GNRs have high current carrying capacity, and better conductive interconnects than CNTs.

4.2 Chemical substitution doping

Chemical substitution doping is a popular method in semiconductor engineering. Many theoretical and several experimental studies for opening up a bandgap were performed in graphene by substitution of a carbon atom by nitrogen [79–86], boron [80,87–89] and combination of them [90,91]. It was found that semimetallic graphene behaviour has been changed to semiconducting one under substitution of carbon by Al or B atoms in a lattice [92].

Nitrogen doping in graphene converts the material into a *p*-type semiconductor. Nitrogen doping has also been established in ZGNRs by CVD process, where it was noticed that at the ribbon edge the dopant atoms prefer to be as far from each other as possible [79]. However, the carrier mobility was significantly lower than expected because of some defects created by the doping.

Doping of a boron atom as a substitution for a graphitic carbon atom is also possible. The presence of a boron atom in the lattice could improve the oxidation resistance of the graphitic carbon, because of the change in the density distribution of the high energy charge carriers [87]. The enhancement of the oxidation resistance is due to the reduction in electron density, which reduces the number of activation sites [87]. In Fig. 6(a), the typical honeycomb alignment of the graphene layer is presented, where one atom of carbon in a matrix is replaced by boron one. Taking into consideration that boron atoms are less electronegative, this doping results in a downward shift of the Fermi level of graphene Fig. 6(b). The boron graphene structure reveals *p*-type semiconducting features with charge particle mobility found to be about 800 $cm^2 \cdot V^{-1} \cdot s^{-1}$. As well as the dopant type (nitrogen or boron), the concentration of dopants and the number of layers of graphene are also major factors which affect the bandgap opening. These changes in bandgap energy (E_g) concerning the concentrations of different dopant atoms are observed from Fig. 6(c).

4.3 Substrate-induced bandgap opening

The scanning tunnel microscope (STM) and scanning tunnel spectroscopy report on bandgap opening in graphene was published in [95]. Epitaxial graphene and *h*-BN also have an experimentally reported bandgap. Experiments using Ni substrate induced a bandgap of 0.5 eV into graphene/*h*-BN hybrid. DFT simulations approach predicted that graphene on bulk *h*-BN and epitaxial grown graphene on copper could induce small changes of bandgap [96]. Moreover, the graphene deposited on SiO_2 developed a bandgap of 0.52 eV [97]. More recently, bandgap opening in epitaxial graphene by SiC was reported [98]. The viability of the growth process of the 2D material and the interaction between the substrate is also interesting. However, the graphene on SiC substrate exhibited *n*-type doping, and the Fermi level shifted above the bandgap. In order to make it a semiconductor, the Fermi level has to move inside the bandgap either by hole doping or by applying a gate voltage [98].

Figure 7 presents the data obtained from angle-resolved

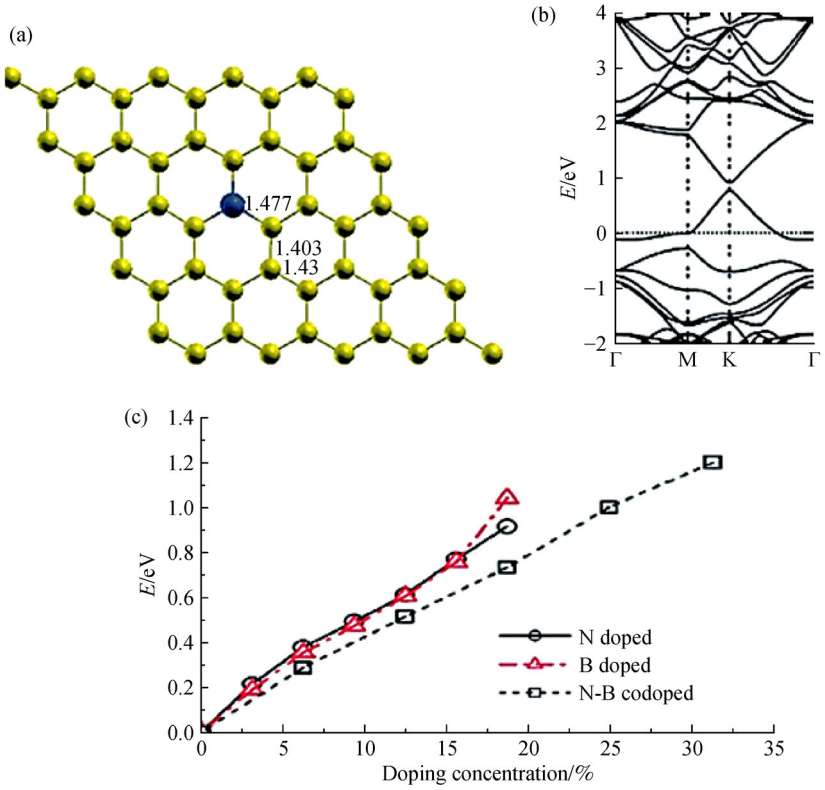

Fig. 6 The effect of the lattice atoms replacement in graphene. (a) Substitution of boron B (blue ball) in graphene; (b) Band structure of a single B-substituted graphene sheet (reproduced with permission from [93]); (c) Variation of the energy gap E_g under N and B atoms substitution, and N–B pair doping concentrations (reproduced with permission from [94])

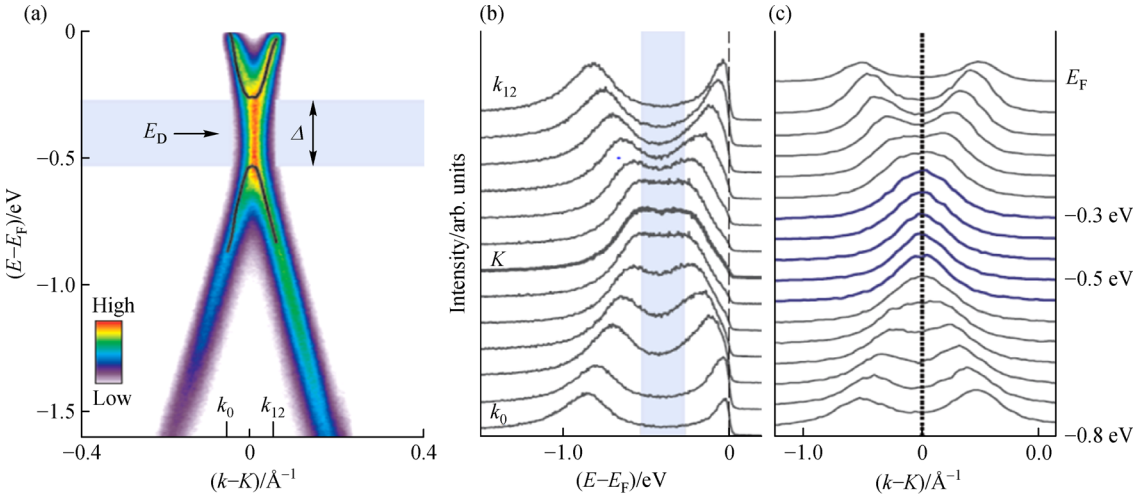

Fig. 7 ARPES intensity maps showing substrate-induced bandgap opening in graphene on SiC. (a) Photoelectron intensity as a function of energy and momentum, for a line through one of the K points; (b) EDC curves showing the dispersion of energy at the K point; (c) MDC showing the no-dispersive peaks at the gap region (Reprinted with permission from the reference [98])

photoemission spectroscopy (ARPES) taken for a line through one of the Dirac points E_D of a single layer graphene on SiC substrate [98]. The photoelectron intensity as a function of energy and the momentum, shown in (Fig. 7(a)), exhibits a dispersion at E_D, that is a characteristic feature of electron-doped graphene. As a result, the valence band and the conduction band are separated by specific energy at the K point. The energy distribution curves (EDCs) demonstrate two peaks at the K point with a minimum energy separation (Fig. 7(b)). In the same energy window, in momentum distribution curves (MDCs) peaks are appearing as non-dispersive (Fig. 7(c)). This supports the existence of a finite bandgap with a conical dispersion. It indicates that the SiC substrate induces the bandgap in epitaxial graphene. Thus, the interaction between the substrate and the graphene layer breaks the sublattice symmetry, leading to a bandgap opening.

4.4 Hybrids

As discussed above, a lot of theoretical studies were carried out for the doping of graphene-like 2D materials with boron and nitrogen to form hybrid structures like BCN (graphene-like boron-carbon-nitrogen monolayers) [99, 100]. Some experimental works reported successful synthesis of BCN materials. BCN atomic hybrids layers with B, C and N contaminants, obtained with the assistance of CVD can exhibit semiconducting behaviour [101]. Quantum molecular dynamics and density functional theory were employed to investigate the structural and electronic properties of carbon and boron nitride sandwich-type hybrid nanoribbons [102]. Structurally stable hybrid systems that behave as semimetals were formed by stacking two zigzag graphene nanoribbons, two zigzag boron nitride nanoribbons [103]. The ZGNRs, which are sandwiched between *h*-BNs, remain in the interfaces of boron nitride sheets and exhibit promising electronic and magnetic properties. The GNRs embedded in boron nitride sheets are potential low-dimensional materials for electronic-spintronic nanodevices [104,105]. The possible applications are further discussed in the next section. The synthesis of large area 2–3 atomic layered graphene films and *h*-BN domains on Cu substrates by chemical vapour deposition also provide a small bandgap opening. Further theoretical investigations predict the increase in a bandgap width with *h*-BN domain size reduction [90]. Hybrid films with tunable and optical properties are therefore prospective candidates for field emission devices [106]. Although the above-discussed methods sound promising, the control over the shape and the domain size is still an unsolved issue. This is essential for the tuning of the bandgap and electronic properties. Thus, a novel method should be introduced for the synthesis and modification of the low-dimensional materials.

5 Plasma tailoring for edge electronics and device fabrication

Plasma-assisted techniques are a perspective method which enables property-tuning with the reaction parameters. In particular, they can assist in synthesising nanostructures and tailoring their physical properties. Moreover, large-scale growth of edge dominated carbon nanostructures (like carbon nanowalls) at low temperature and pressure is possible using plasma-assisted techniques. Beside this, a simple plasma modification of materials, frequently used in microelectronics, offers new possibilities for tailoring 2D material properties, which can lead to

the rise of edge electronics. The possibilities of tailoring material vacancies, adatoms like gold, and the exchange of single atoms and the modifications of grain boundaries will induce a reasonable change in electrical conductivity and transport behaviours [107,108]. Some of these remarkable modifications with plasma generated in different gases, which are used to enhance the electrical properties of 2D nanomaterials are discussed here and summarised in Table 2.

Plasma-assisted nitrogen functionalisation enhances the electrical properties by lowering the work function of electrons in nanomaterial. Apart from this, modifications can also be done to the structures like nanowalls or nanoribbons, in order to implement those into nanodevices like field effect transistors [77]. In 2008, Stampfer et al. fabricated a fully tunable graphene single electron transistor based on an etched-width-modulated graphene nanostructure [123]. In this case, N_2 plasma was used to reduce the work function of material from 4.91 to 4.37 eV [124]. Similarly, a controlled edge nitrogen functionalisation can also be done with NH_3 plasma. A result of such nitrogen incorporation process increases the nanomaterial specific capacitance (280 F/g), which can enable the preparation of electrodes for novel ultra-supercapacitors [125].

Furthermore, the processing with O_2 plasma causes the bandgap opening and thereby increased material responses towards electrochemical activities, which can be used in optoelectronic devices, actuators and patterning of flexible transparent electrodes [126–128]. Simultaneous reduction and defect restoration of graphene oxide nanoribbon (GONR) via plasma-assisted chemistry was demonstrated by Chiang et al. [129]. When H_2 and CH_4 gases are used, the atomic hydrogen or/and carbon-containing ions and radicals are generated by molecule dissociation and ionisation in plasma. Such plasmas are convenient for removal of oxygen atoms or oxygen functional groups like in the case of GONR films. The synergistic effect of simultaneous reduction and defect restoration on GONR was achieved with the plasma gas mixture H_2/CH_4 treatment [130,131]. The results of this study indicate that the optical energy gap of the treated reduced-GONR (r-GONR) can be engineered by controlling the plasma exposure time. Furthermore, the conductivity of the GONR can be enhanced as well. This unique plasma reduction is characterised by short processing times, high purity of obtained nanomaterial and low temperature compared with conventional thermal and chemical reductions. Therefore such non-equilibrium chemical processing approach can be used more widely beyond the mere reduction of GONR and graphene oxide (GO).

Similarly to graphene, numerous investigations were performed in 2D heterostructured MoS_2, one of the most promising candidates for field effect transistors (FET), where the influence of point defects, dislocations, grain boundaries are considered [132–134]. Liu et al. [135] investigated the defects and the electronic band structure in MoS_2 and showed that the sulphur vacancies lead to the pinning of Fermi level near the conduction band. The defect formed by the sulphur vacancies induced an *n*-type behaviour in MoS_2. Later, Qiu et al. [136] confirmed this effect by introducing localised electron donor states inside the bandgap. Hong et al. reported a low-temperature doping method [137] for reparation of the sulphur vacancies in MoS_2 layers. Islam et al. described tuning of electrical properties via defect engineering using oxygen

Table 2 Plasma-assisted tailoring of 2D materials for electrical properties and their applications

Carrier gas	Change in material	Applications
NH_3	Yielding graphene quantum nanosheets [109]	Gas sensors
N_2/H_2	Incorporation of nitrogen preferably at the edges [110]	FETs
N_2/O_3	Defect generation	Supercapacitors
O_2	Control of thermal boundary conductance [111] Narrowing the bandgap from 6.0 eV to 4.3 eV (in *h*-BN) [112] Sulphur vacancy engineering in MoS_2 [113]	Lithium batteries
Ar/O_2	Wettability and surface energy [114]	
Ar/H_2	Conversion of sp^2 to sp^3 hybridisation (opening a bandgap of 3.5 eV) [115], defects and disorder generation	
C_3H_9B	*p*-Type conductivity with an on-off ratio of 10^2 [116], tunable bandgap ranging from 0 to ~0.54 eV	Rectifying diodes
CF_4 SF_6 Ar/SF_6 CHF_3	*p*-Type doping for gas sensing (e.g., NH_3) [117]	Back-gated FETs Multi-bit memory transistors Photodiodes Hydrogen production
Cl_2	*p*-Type doping increases carrier mobility [118]	Sensors
H_2	*p*-Type doping in MoS_2 [119], reverse fluorination in WS_2 [117]	Photovoltaic devices
CH_4	The transition of insulating to semiconducting [120]	
PH_3/He	Minimised etching and low damage [121]	
N_2	Substitution of sulphur with nitrogen in MoS_2 [122]	

plasma [138]. Further experiments [127,139,140] revealed that plasma could play an important role in surface functionalisation, exchange of atoms and bandgap opening, as described before. The current state-of-the-art in plasma surface tailoring is presented in Table 2. The table summarises potential plasmas generated from proposed gas or gas mixtures for modification of 2D materials and their applications in functionalised nanoelectronics devices.

Doping with boron is done with boron-containing plasma typically generated in gases or vapours. An example of such process is doping of the zigzag edged graphene nanoribbons [141]. The obtained nanoribbons exhibit a half-metallicity beyond the particular electric field, which can lead to potential applications in spintronics and semiconductor devices [88]. The armchair nanoribbons, which are substitutionally doped, can be metalised by 7 boron atom clusters (B7). However, this doping achieved merely in small quantities is significant only for very thin 2D structures. Theoretical studies on the doping and transport properties for large area graphene predict that their transport properties are not significantly affected even at 4% doping levels. The quantum interference would be minimised, and thus the carrier mobilities would become more asymmetric only at higher doping values [83]. The experimental investigations of boron and nitrogen doped graphene, which were synthesised in arc discharge of diborane/hydrogen gas mixture [80] confirmed that they exhibit *p*-type and *n*-type semiconducting properties. This behaviour could be systematically tuned by varying the concentrations of boron and nitrogen in the gas mixture. However, the doping of boron creates defects and disorders in graphene layers. This was observed with STM and Raman analyses by Endo et al. [142]. In this context, plasma-assisted techniques are more suitable for the synthesis and defect engineering in graphene sheets as well as in narrow structures like nanoribbons.

When the edge of 2D nanostructures is considered, one can expect different behaviours depending on external influence as well. Taking graphene as a model example, the current flow throughout the two-dimensional plane, as in a regular conductor. This behaviour could be changed with plasma assistance or by applying a magnetic field. Under a magnetic field perpendicular to the graphene plane, the current flows only along the edges in a direction depending on the orientation of the magnetic field [143]. This common phenomenon is often referred to as quantum Hall effect [144]. However, Young et al. came up with an unexpected phenomenon beyond Hall effect [145]. The researchers applied a second powerful magnetic field in the same direction of the graphene flake. The experiment ended up in the electron motion around the edge in any direction (either in clockwise or anticlockwise). In particular, the electrons with one kind of spin move in a clockwise direction and at the same time the electrons with the opposite spins move counter clockwise. That literarily means a conductive edge or a circuit. This also indicates a possibility that 2D nanostructures like graphene can be topological insulators. Unlike in conventional topological insulators, the above-mentioned circuit in graphene can be controlled by varying the magnetic field. Another benefit of this is the inhibition of backscattering, which would interrupt the motion of the electrons. As a result, the imperfections in the material do not affect electron motion, since the electrons can travel along the edges irrespectively. However, the spin-dependent behaviour at the newly developed edge states can be modified with plasma, e.g., doping of gold atoms to the edges. Plasma itself as a tool can selectively dope the material with atoms like gold or nitrogen. In the case of gold, it is expected the conductivity of the material will increase. However, in this case, the inserted atoms would decrease the conductance. The gold atoms added into the graphene edges, namely allow the electrons to backscatter into the oppositely travelling states, and thereby the mixing of the electron spins [145,146]. Moreover, there is also a possibility to control the conductivity along the edges with the concentrations of the gold atoms. The idea for further research is to create the circuit based on edge dominating 2D material, which are, in turn, doped with a noble metal. This can be done by using suitable plasma (Ar or N) in order to incorporate gold atoms into the edges of graphene nanoribbons (see Fig. (8)). And more, under the influence of high magnetic fields with different orientations, a spin depended current flow is expected to be obtained along the edges in the closed electrical circuit designed with Au modified nanoribbons.

However, the device fabrication is another challenge, because the scalable deposition of high-quality Ohmic contacts is a problem that needs to be further improved. Successful strategies *in situ* involve the deposition of pure metal contacts, such as Au and Pd, under ultra-high vacuum or patterning/surface treatment of the area under the contact. It facilitates to create stronger interaction between 2D surface and the metal. Etching of 2D materials is also an issue, but mild plasma-assisted methods would help to solve this problem. Controlled etching of 2D materials is critical to achieving sophisticated device structures such as LEDs, tunnel transistors and for side contacts. The relatively mature technologies, such as plasma, can therefore easily be tuned to etch stacks of 2D layers with profiles for device architecture. The emerging field of Atomic Layer Etching (ALE) of both conventional and 2D materials could contribute to further advances in atomic scale devices. However, all these device fabrication processes are beyond the review of this paper.

6 Conclusions

The mini-review summarises existing efforts on tailoring electrical properties of 2D structured nanomaterials with

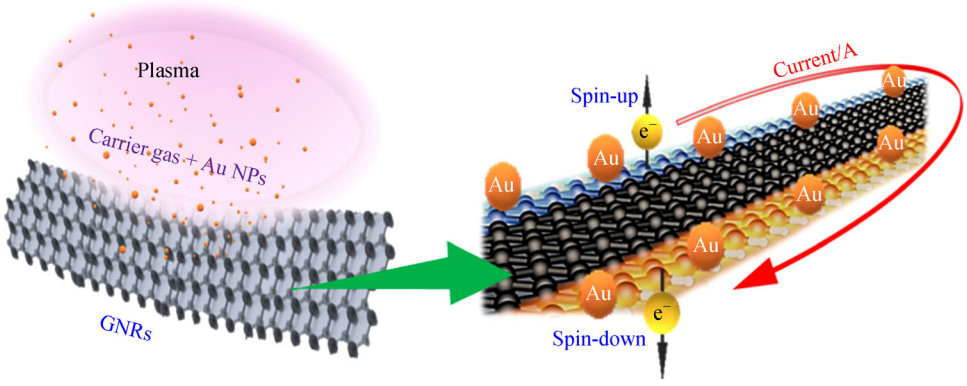

Fig. 8 Schematic representation of graphene NRs edge tailoring with the assistance of plasma for 2D functionalisation electronics. Electrons on the two zigzag edges exhibit opposite directions of rotation (spin)-'spin-down' on the bottom edge or 'spin-up' on the top edge that generates a current flow

plasma chemistry, which are aimed at possible applications of these materials for electrical and optoelectronic devices. Many different plasma techniques have been used for enhancing their conductivity and other electrical properties. In this context, the significance of the surface, as well as the edges of the 2D structures, were studied. Namely, the edges are becoming of utmost significance for designing nanoelectronics. One can tailor these 2D materials and structures like nanoribbons, nanowalls and nanosheets by selective doping of adatoms (metallic or non-metallic) like gold and nitrogen**,** defect engineering or by applying external magnetic or electric field. Plasma-based methods enable controlled, and selective functionalisation of the selected materials and various plasma species like N_2, O_2, B, etc. Further enhancement of material properties can be achieved by controlling the morphology like the width of nanostructures including nanoribbons and nanowalls. Moreover, plasma can support the growth or synthesis as well as modifications of new 2D hybrid structures. With these processes, we can create new emerging functionalised 2D materials for nanoelectronics, which are featured by quantum conductivity. This will lead to miniaturisation of electrical circuits, which will contribute to engineer high-performance next-generation 2D electronic functional devices with significantly reduced energy consumption. The biggest breakthrough in this, we believe will occur due on edge-dominated 2D nanostructures.

References

1. Tiwari J N, Tiwari R N, Kim K S. Zero-dimensional, one-dimensional, two-dimensional and three-dimensional nanostructured materials for advanced electrochemical energy devices. Progress in Materials Science, 2012, 57(4): 724–803
2. Novoselov K S, Geim A K, Morozov S V, Jiang D, Katsnelson M, Grigorieva I, Dubonos S V, Firsov A A. Two-dimensional gas of massless Dirac fermions in graphene. Nature, 2005, 438(7065): 197–200
3. Dutta S, Pati S K. Novel properties of graphene nanoribbons: A review. Journal of Materials Chemistry, 2010, 20(38): 8207–8223
4. Li Y, Jiang X, Liu Z, Liu Z. Strain effects in graphene and graphene nanoribbons: The underlying mechanism. Nano Research, 2010, 3(8): 545–556
5. Pereira V M, Neto A C. Strain engineering of graphene's electronic structure. Physical Review Letters, 2009, 103(4): 046801
6. Bhimanapati G R, Lin Z, Meunier V, Jung Y, Cha J, Das S, Xiao D, Son Y, Strano M S, Cooper V R, et al. Recent advances in two-dimensional materials beyond graphene. ACS Nano, 2015, 9(12): 11509–11539
7. Mas-Balleste R, Gomez-Navarro C, Gomez-Herrero J, Zamora F. 2D Materials: To graphene and beyond. Nanoscale, 2011, 3(1): 20–30
8. Mak K F, Lee C, Hone J, Shan J, Heinz T F. Atomically thin MoS_2: A new direct-gap semiconductor. Physical Review Letters, 2010, 105(13): 136805
9. Lukowski M A, Daniel A S, English C R, Meng F, Forticaux A, Hamers R J, Jin S. Highly active hydrogen evolution catalysis from metallic WS_2 nanosheets. Energy & Environmental Science, 2014, 7(8): 2608–2613
10. Andriotis A N, Menon M. Tunable magnetic properties of transition metal doped MoS_2. Physical Review B, 2014, 90(12): 125304
11. He J, Hummer K, Franchini C. Stacking effects on the electronic and optical properties of bilayer transition metal dichalcogenides MoS_2, $MoSe_2$, WS_2, and WSe_2. Physical Review B, 2014, 89(7): 075409
12. Wang Q H, Kalantar-Zadeh K, Kis A, Coleman J N, Strano M S. Electronics and optoelectronics of two-dimensional transition metal dichalcogenides. Nature Nanotechnology, 2012, 7(11): 699–712
13. Cao L, Yang S, Gao W, Liu Z, Gong Y, Ma L, Shi G, Lei S, Zhang Y, Zhang S, Vajtai R, Ajayan P M. Direct laser-patterned micro-supercapacitors from paintable MoS_2 films. Small, 2013, 9(17): 2905–2910
14. Huang Y H, Peng C C, Chen R S, Huang Y S, Ho C H. Transport

properties in semiconducting NbS_2 nanoflakes. Applied Physics Letters, 2014, 105(9): 093106
15. Moore D B, Beekman M, Disch S, Zschack P, Häusler I, Neumann W, Johnson D C. Synthesis, structure, and properties of turbostratically disordered $(PbSe)1.18(TiSe_2)_2$. Chemistry of Materials, 2013, 25(12): 2404–2409
16. Jeong S, Yoo D, Jang J T, Kim M, Cheon J. Well-defined colloidal 2-D layered transition-metal chalcogenide nanocrystals via generalized synthetic protocols. Journal of the American Chemical Society, 2012, 134(44): 18233–18236
17. Yu Z, Tetard L, Zhai L, Thomas J. Supercapacitor electrode materials: Nanostructures from 0 to 3 dimensions. Energy & Environmental Science, 2015, 8(3): 702–730
18. Hsu Y K, Chen Y C, Lin Y G, Chen L C, Chen K H. Birnessite-type manganese oxides nanosheets with hole acceptor assisted photoelectrochemical activity in response to visible light. Journal of Materials Chemistry, 2012, 22(6): 2733–2739
19. Geim A K, Grigorieva I V. Van der Waals heterostructures. Nature, 2013, 499(7459): 419–425
20. Eda G, Fujita T, Yamaguchi H, Voiry D, Chen M, Chhowalla M. Coherent atomic and electronic heterostructures of single-layer MoS_2. ACS Nano, 2012, 6(8): 7311–7317
21. Li H, Lu G, Wang Y, Yin Z, Cong C, He Q, Wang L, Ding F, Yu T, Zhang H. Mechanical exfoliation and characterization of single- and few- layer nanosheets of WSe_2, TaS_2, and $TaSe_2$. Small, 2013, 9(11): 1974–1981
22. Li H, Lu G, Yin Z, He Q, Li H, Zhang Q, Zhang H. Optical identification of single- and few- layer MoS_2 sheets. Small, 2012, 8 (5): 682–686
23. Tongay S, Zhou J, Ataca C, Lo K, Matthews T S, Li J, Grossman J C, Wu J. Thermally driven crossover from indirect toward direct bandgap in 2D semiconductors: $MoSe_2$ versus MoS_2. Nano Letters, 2012, 12(11): 5576–5580
24. Wang F, Wang Z, Wang Q, Wang F, Yin L, Xu K, Huang Y, He J. Synthesis, properties and applications of 2D non-graphene materials. Nanotechnology, 2015, 26(29): 292001 1–7
25. Xu Y, Liu Z, Zhang X, Wang Y, Tian J, Huang Y, Ma Y, Zhang X, Chen Y. A graphene hybrid material covalently functionalized with porphyrin: Synthesis and optical limiting property. Advanced Materials, 2009, 21(12): 1275–1279
26. Avouris P. Graphene: Electronic and photonic properties and devices. Nano Letters, 2010, 10(11): 4285–4294
27. Xu C, Xu B, Gu Y, Xiong Z, Sun J, Zhao X S. Graphene-based electrodes for electrochemical energy storage. Energy & Environmental Science, 2013, 6(5): 1388–1414
28. Huang Y, Liang J, Chen Y. An overview of the applications of graphene-based materials in supercapacitors. Small, 2012, 8(12): 1805–1834
29. Lv W, Li Z, Deng Y, Yang Q H, Kang F. Graphene-based materials for electrochemical energy storage devices: Opportunities and challenges. Energy Storage Materials, 2016, 2(1): 107–138
30. Fratini S, Guinea F. Substrate-limited electron dynamics in graphene. Physical Review B, 2008, 77(19): 195415
31. Prezzi D, Eom D, Rim K T, Zhou H, Lefenfeld M, Xiao S, Nuckolls C, Heinz T F, Flynn G W, Hybertsen M S. Edge structures for nanoscale graphene islands on Co (0001) surfaces. ACS Nano, 2014, 8(6): 5765–5773
32. Liu H, Zhang X, Zhai T, Sander T, Chen L, Klar P J. Centimeter-scale-homogeneous SERS substrates with seven-order global enhancement through thermally controlled plasmonic nanostructures. Nanoscale, 2014, 6(10): 5099–5105
33. Israr-Qadir M, Jamil-Rana S, Nur O, Willander M, Larsson L A, Holtz P O. Fabrication of ZnO nanodisks from structural transformation of ZnO nanorods through natural oxidation and their emission characteristics. Ceramics International, 2014, 40(1): 2435–2439
34. Wang H, Guo Z, Wang S, Liu W. One-dimensional titania nanostructures: Synthesis and applications in dye-sensitized solar cells. Thin Solid Films, 2014, 558: 1–19
35. Yu X Y, Feng Y, Guan B, Lou X W D, Paik U. Carbon coated porous nickel phosphides nanoplates for highly efficient oxygen evolution reaction. Energy & Environmental Science, 2016, 9(4): 1246–1250
36. Peng L, Feng Y, Bai Y, Qiu H J, Wang Y. Designed synthesis of hollow Co_3O_4 nanoparticles encapsulated in a thin carbon nanosheet array for high and reversible lithium storage. Journal of Materials Chemistry. A, Materials for Energy and Sustainability, 2015, 3(16): 8825–8831
37. Karakouz T, Holder D, Goomanovsky M, Vaskevich A, Rubinstein I. Morphology and refractive index sensitivity of gold island films. Chemistry of Materials, 2009, 21(24): 5875–5885
38. Hiramatsu M, Shiji K, Amano H, Hori M. Fabrication of vertically aligned carbon nanowalls using capacitively coupled plasma-enhanced chemical vapor deposition assisted by hydrogen radical injection. Applied Physics Letters, 2004, 84(23): 4708–4710
39. Kargar A, Jing Y, Kim S J, Riley C T, Pan X, Wang D. ZnO/CuO heterojunction branched nanowires for photoelectrochemical hydrogen generation. ACS Nano, 2013, 7(12): 11112–11120
40. Terrones H, Lv R, Terrones M, Dresselhaus M S. The role of defects and doping in 2D graphene sheets and 1D nanoribbons. Reports on Progress in Physics, 2012, 75(6): 062501
41. Zhang X, Wang X B, Wang L W, Wang W K, Long L L, Li W W, Yu H Q. Synthesis of a highly efficient BiOCl single-crystal nanodisk photocatalyst with exposing {001} facets. ACS Applied Materials & Interfaces, 2014, 6(10): 7766–7772
42. Gao R, Yin L, Wang C, Qi Y, Lun N, Zhang L, Liu Y, Kang L, Wang X. High-yield synthesis of boron nitride nanosheets with strong ultraviolet cathodoluminescence emission. Journal of Physical Chemistry C, 2009, 113(34): 15160–15165
43. Inamdar A I, Kim J, Jo Y, Woo H, Cho S, Pawar S M, Lee S, Gunjakar J, Cho Y, Hou B, et al. Highly efficient electro-optically tunable smart-supercapacitors using an oxygen-excess nanograin tungsten oxide thin film. Solar Energy Materials and Solar Cells, 2017, 166: 78–85
44. Qu Y, Shao M, Shao Y, Yang M, Xu J, Kwok C T, Shi X, Lu Z, Pan H. Ultra-high electrocatalytic activity of VS_2 nanoflowers for efficient hydrogen evolution reaction. Journal of Materials Chemistry. A, Materials for Energy and Sustainability, 2017, 5 (29): 15080–15086
45. Tao J, Guan L. Tailoring the electronic and magnetic properties of monolayer SnO by B, C, N, O and F adatoms. Scientific Reports, 2017, 7: 44568

46. Terrones M, Botello-Méndez A R, Campos-Delgado J, López-Urías F, Vega-Cantú Y I, Rodríguez-Macías F J, Elias Arriaga A L, Muñoz-Sandoval E, Cano-Márquez A G, Charlier J C, et al. Graphene and graphite nanoribbons: Morphology, properties, synthesis, defects and applications. Nano Today, 2010, 5(4): 351–372
47. Kosynkin D V, Higginbotham A L, Sinitskii A, Lomeda J R, Dimiev A, Price B K, Tour J M. Longitudinal unzipping of carbon nanotubes to form graphene nanoribbons. Nature, 2009, 458 (7240): 872–876
48. Li L. Epitaxial Graphene on SiC(0001): More Than Just Honeycombs, Physics and Applications of Graphene-Experiments. Sergey M, ed. Rijeka: InTech Europe, 2011, 55–72
49. Lee Y H, Zhang X Q, Zhang W, Chang M T, Lin C T, Chang K D, Yu Y C, Wang J T, Chang C S, Li L J, et al. Synthesis of large-area MoS_2 atomic layers with chemical vapor deposition. Advanced Materials, 2012, 24(17): 2320–2325
50. Zhao J, Pei S, Ren W, Gao L, Cheng H M. Efficient preparation of large-area graphene oxide sheets for transparent conductive films. ACS Nano, 2010, 4(9): 5245–5252
51. Sols F, Guinea F, Neto A C. Coulomb blockade in graphene nanoribbons. Physical Review Letters, 2007, 99(16): 166803
52. Jiao L, Zhang L, Wang X, Diankov G, Dai H. Narrow graphene nanoribbons from carbon nanotubes. Nature, 2009, 458(7240): 877–880
53. Bai J, Huang Y. Fabrication and electrical properties of graphene nanoribbons. Materials Science and Engineering R Reports, 2010, 70(3-6): 341–353
54. Li Z, Qian H, Wu J, Gu B L, Duan W. Role of symmetry in the transport properties of graphene nanoribbons under bias. Physical Review Letters, 2008, 100(20): 206802
55. Boutahir M, El Majdoub S, Rahmani A H, Fakrach B, Chadli H, Rahmani A. Electronic properties of phosphorene nanoribbons. Energy Procedia, 2017, 139: 207–210
56. Ning W, Kong F, Xi C, Graf D, Du H, Han Y, Yang J, Yang K, Tian M, Zhang Y. Evidence of topological two-dimensional metallic surface states in thin bismuth nanoribbons. ACS Nano, 2014, 8(7): 7506–7512
57. Liang G, Neophytou N, Nikonov D E, Lundstrom M S. Performance projections for ballistic graphene nanoribbon field-effect transistors. IEEE Transactions on Electron Devices, 2007, 54 (4): 677–682
58. Chen J H, Jang C, Adam S, Fuhrer M S, Williams E D, Ishigami M. Charged-impurity scattering in graphene. Nature Physics, 2008, 4 (5): 377–381
59. Obradovic B, Kotlyar R, Heinz F, Matagne P, Rakshit T, Giles M D, Nikonov D E. Analysis of graphene nanoribbons as a channel material for field-effect transistors. Applied Physics Letters, 2006, 88(14): 142102
60. Wang X, Ouyang Y, Li X, Wang H, Guo J, Dai H. Room-temperature all-semiconducting sub-10-nm graphene nanoribbon field-effect transistors. Physical Review Letters, 2008, 100(20): 206803
61. Liao L, Bai J, Lin Y C, Qu Y, Huang Y, Duan X. High-performance top-gated graphene-nanoribbon transistors using zirconium oxide nanowires as high-dielectric-constant gate dielectrics. Advanced Materials, 2010, 22(17): 1941–1945
62. Tapasztó L, Dobrik G, Lambin P, Biró L P. Tailoring the atomic structure of graphene nanoribbons by scanning tunnelling microscope lithography. Nature Nanotechnology, 2008, 3(7): 397–401
63. Özyilmaz B, Jarillo-Herrero P, Efetov D, Kim P. Electronic transport in locally gated graphene nanoconstrictions. Applied Physics Letters, 2007, 91(19): 192107
64. Yazdanpanah A, Pourfath M, Fathipour M, Kosina H, Selberherr S. A numerical study of line-edge roughness scattering in graphene nanoribbons. IEEE Transactions on Electron Devices, 2012, 59(2): 433–440
65. Gunlycke D, Areshkin D A, White C T. Semiconducting graphene nanostrips with edge disorder. Applied Physics Letters, 2007, 90 (14): 142104
66. Evaldsson M, Zozoulenko I V, Xu H, Heinzel T. Edge-disorder-induced Anderson localization and conduction gap in graphene nanoribbons. Physical Review. B, 2008, 78(16): 161407
67. Querlioz D, Apertet Y, Valentin A, Huet K, Bournel A, Galdin-Retailleau S, Dollfus P. Suppression of the orientation effects on bandgap in graphene nanoribbons in the presence of edge disorder. Applied Physics Letters, 2008, 92(4): 042108
68. Gutiérrez C, Brown L, Kim C J, Park J, Pasupathy A N. Klein tunnelling and electron trapping in nanometre-scale graphene quantum dots. Nature Physics, 2016, 12(11): 1069
69. Ponomarenko L A, Schedin F, Katsnelson M I, Yang R, Hill E W, Novoselov K S, Geim A K. Chaotic Dirac billiard in graphene quantum dots. Science, 2008, 320(5874): 356–358
70. Stampfer C, Güttinger J, Molitor F, Graf D, Ihn T, Ensslin K. Tunable Coulomb blockade in nanostructured graphene. Applied Physics Letters, 2008, 92(1): 012102
71. Bischoff D, Varlet A, Simonet P, Eich M, Overweg H C, Ihn T, Ensslin K. Localized charge carriers in graphene nanodevices. Applied Physics Reviews, 2015, 2(3): 031301
72. Novoselov K S, Geim A K, Morozov S V, Jiang D A, Zhang Y, Dubonos S V, Grigorieva I V, Firsov A A. Electric field effect in atomically thin carbon films. Science, 2004, 306(5696): 666–669
73. Novoselov K S, Neto A C. Two-dimensional crystals-based heterostructures: Materials with tailored properties. Physica Scripta, 2012, T146: 014006
74. Nakada K, Fujita M, Dresselhaus G, Dresselhaus M S. Edge state in graphene ribbons: Nanometer size effect and edge shape dependence. Physical Review. B, 1996, 54(24): 17954
75. Wakabayashi K. Electronic transport properties of nanographite ribbon junctions. Physical Review. B, 2001, 64(12): 125428
76. Fujita M, Wakabayashi K, Nakada K, Kusakabe K. Peculiar localized state at zigzag graphite edge. Journal of the Physical Society of Japan, 1996, 65(7): 1920–1923
77. Li X, Wang X, Zhang L, Lee S, Dai H. Chemically derived, ultrasmooth graphene nanoribbon semiconductors. Science, 2008, 319(5867): 1229–1232
78. Berger C, Song Z, Li X, Wu X, Brown N, Naud C, Mayou D, Li T, Hass J, Marchenkov A N, et al. Electronic confinement and coherence in patterned epitaxial graphene. Science, 2006, 312 (5777): 1191–1196
79. Wei D, Liu Y, Wang Y, Zhang H, Huang L, Yu G. Synthesis of *N*-

doped graphene by chemical vapor deposition and its electrical properties. Nano Letters, 2009, 9(5): 1752–1758
80. Panchakarla L S, Subrahmanyam K S, Saha S K, Govindaraj A, Krishnamurthy H R, Waghmare U V, Rao C N R. Synthesis, structure, and properties of boron- and nitrogen- doped graphene. Advanced Materials, 2009, 21(46): 4726–4730
81. Yu S S, Zheng W T, Wen Q B, Jiang Q. First principle calculations of the electronic properties of nitrogen-doped carbon nanoribbons with zigzag edges. Carbon, 2008, 46(3): 537–543
82. Li Y, Zhou Z, Shen P, Chen Z. Spin gapless semiconductor−metal−half-metal properties in nitrogen-doped zigzag graphene nanoribbons. ACS Nano, 2009, 3(7): 1952–1958
83. Lherbier A, Blase X, Niquet Y M, Triozon F, Roche S. Charge transport in chemically doped 2D graphene. Physical Review Letters, 2008, 101(3): 036808
84. Zheng X H, Rungger I, Zeng Z, Sanvito S. Effects induced by single and multiple dopants on the transport properties in zigzag-edged graphene nanoribbons. Physical Review. B, 2009, 80(23): 235426
85. Peköz R, Erkoç Ş. A theoretical study of chemical doping and width effect on zigzag graphene nanoribbons. Physica E, Low-Dimensional Systems and Nanostructures, 2009, 42(2): 110–115
86. Shao Y, Zhang S, Engelhard M H, Li G, Shao G, Wang Y, Liu J, Aksay I A, Lin Y. Nitrogen-doped graphene and its electrochemical applications. Journal of Materials Chemistry, 2010, 20 (35): 7491–7496
87. Ma X, Wang Q, Chen L Q, Cermignani W, Schobert H H, Pantano C G. Semi-empirical studies on electronic structures of a boron-doped graphene layer—implications on the oxidation mechanism. Carbon, 1997, 35(10-11): 1517–1525
88. Dutta S, Pati S K. Half-metallicity in undoped and boron doped graphene nanoribbons in the presence of semilocal exchange-correlation interactions. Journal of Physical Chemistry B, 2008, 112(5): 1333–1335
89. Panchakarla L S, Govindaraj A, Rao C N R. Boron-and nitrogen-doped carbon nanotubes and graphene. Inorganica Chimica Acta, 2010, 363(15): 4163–4174
90. Ci L, Song L, Jin C, Jariwala D, Wu D, Li Y, Srivastava A, Wang Z F, Storr K, Balicas L, et al. Atomic layers of hybridized boron nitride and graphene domains. Nature Materials, 2010, 9(5): 430–435
91. Drost R, Uppstu A, Schulz F, Hämäläinen S K, Ervasti M, Harju A, Liljeroth P. Electronic states at the graphene-hexagonal boron nitride zigzag interface. Nano Letters, 2014, 14(9): 5128–5132
92. Nigar S, Zhou Z, Wang H, Imtiaz M. Modulating the electronic and magnetic properties of graphene. RSC Advances, 2017, 7(81): 51546–51580
93. Rani P, Jindal V K. Designing band gap of graphene by B and N dopant atoms. RSC Advances, 2013, 3(3): 802–812
94. Nath P, Chowdhury S, Sanyal D, Jana D. Ab-initio calculation of electronic and optical properties of nitrogen and boron doped graphene nanosheet. Carbon, 2014, 73: 275–282
95. Kawasaki T, Ichimura T, Kishimoto H, Akbar A A, Ogawa T, Oshima C. Double atomic layers of graphene/monolayer h-BN on Ni (111) studied by scanning tunneling microscopy and scanning tunneling spectroscopy. Surface Review and Letters, 2002, 9(3-4): 1459–1464
96. Giovannetti G, Khomyakov P A, Brocks G, Kelly P J, Van Den Brink J. Substrate-induced band gap in graphene on hexagonal boron nitride: Ab initio density functional calculations. Physical Review. B, 2007, 76(7): 073103
97. Shemella P, Nayak S K. Electronic structure and band-gap modulation of graphene via substrate surface chemistry. Applied Physics Letters, 2009, 94(3): 032101
98. Zhou S Y, Gweon G H, Fedorov A V, First P D, De Heer W A, Lee D H, Guinea F, Castro Neto A H, Lanzara A. Substrate-induced bandgap opening in epitaxial graphene. Nature Materials, 2007, 6 (10): 770–775
99. Liu A Y, Wentzcovitch R M, Cohen M L. Atomic arrangement and electronic structure of BC2N. Physical Review. B, 1989, 39(3): 1760
100. Miyamoto Y, Rubio A, Cohen M L, Louie S G. Chiral tubules of hexagonal BC2N. Physical Review. B, 1994, 50(7): 4976
101. Liang Y, Kawazoe Y. Half-metallicity modulation of hybrid BN-C nanotubes by external electric fields: A first-principles study. Journal of Chemical Physics, 2014, 140(23): 234702
102. Huang Y, Bando Y, Tang C, Zhi C, Terao T, Dierre B, Sekiguchi T, Golberg D. Thin-walled boron nitride microtubes exhibiting intense band-edge UV emission at room temperature. Nanotechnology, 2009, 20(8): 085705
103. Silva F W N, Cruz-Silva E, Terrones M, Terrones H, Barros E B. BNC nanoshells: A novel structure for atomic storage. Nanotechnology, 2017, 28(46): 465201
104. Ding Y, Wang Y, Ni J. Electronic properties of graphene nanoribbons embedded in boron nitride sheets. Applied Physics Letters, 2009, 95(12): 123105
105. Kim W Y, Choi Y C, Kim K S. Understanding structures and electronic/spintronic properties of single molecules, nanowires, nanotubes, and nanoribbons towards the design of nanodevices. Journal of Materials Chemistry, 2008, 18(38): 4510–4521
106. D'Innocenzo V, Srimath Kandada A R, De Bastiani M, Gandini M, Petrozza A. Tuning the light emission properties by band gap engineering in hybrid lead halide perovskite. Journal of the American Chemical Society, 2014, 136(51): 17730–17733
107. Seifert M, Vargas J E, Bobinger M, Sachsenhauser M, Cummings A W, Roche S, Garrido J A. Role of grain boundaries in tailoring electronic properties of polycrystalline graphene by chemical functionalization. 2D Materials, 2015, 2(2): 024008
108. Chow P K, Jacobs-Gedrim R B, Gao J, Lu T M, Yu B, Terrones H, Koratkar N. Defect-induced photoluminescence in monolayer semiconducting transition metal dichalcogenides. ACS Nano, 2015, 9(2): 1520–1527
109. Moon J, An J, Sim U, Cho S P, Kang J H, Chung C, Seo J H, Lee J, Nam K T, Hong B H. One-step synthesis of *N*-doped graphene quantum sheets from monolayer graphene by nitrogen plasma. Advanced Materials, 2014, 26(21): 3501–3505
110. Kato T, Jiao L, Wang X, Wang H, Li X, Zhang L, Hatakeyama R, Dai H. Room-temperature edge functionalization and doping of graphene by mild plasma. Small, 2011, 7(5): 574–577
111. Foley B M, Hernández S C, Duda J C, Robinson J T, Walton S G, Hopkins P E. Modifying surface energy of graphene via plasma-based chemical functionalization to tune thermal and electrical

transport at metal interfaces. Nano Letters, 2015, 15(8): 4876–4882
112. Singh R S. Influence of oxygen impurity on electronic properties of carbon and boron nitride nanotubes: A comparative study. AIP Advances, 2015, 5(11): 117150
113. Nan H, Wang Z, Wang W, Liang Z, Lu Y, Chen Q, He D, Tan P, Miao F, Wang X, et al. Strong photoluminescence enhancement of MoS_2 through defect engineering and oxygen bonding. ACS Nano, 2014, 8(6): 5738–5745
114. Shin Y J, Wang Y, Huang H, Kalon G, Wee A T S, Shen Z, Bhatia C S, Yang H. Surface-energy engineering of graphene. Langmuir, 2010, 26(6): 3798–3802
115. Elias D C, Nair R R, Mohiuddin T M G, Morozov S V, Blake P, Halsall M P, Ferrari A C, Boukhvalov D W, Katsnelson M I, Geim A K, et al. Control of graphene's properties by reversible hydrogenation: Evidence for graphane. Science, 2009, 323 (5914): 610–613
116. Tang Y B, Yin L C, Yang Y, Bo X H, Cao Y L, Wang H E, Zhang W J, Bello I, Lee S T, Cheng H M, et al. Tunable band gaps and *p*-type transport properties of boron-doped graphenes by controllable ion doping using reactive microwave plasma. ACS Nano, 2012, 6(3): 1970–1978
117. Jhon Y I, Kim Y, Park J, Kim J H, Lee T, Seo M, Jhon Y M. Significant exciton brightening in monolayer tungsten disulfides via fluorination: *n*-Type gas sensing semiconductors. Advanced Functional Materials, 2016, 26(42): 7551–7559
118. Zhang X, Hsu A, Wang H, Song Y, Kong J, Dresselhaus M S, Palacios T. Impact of chlorine functionalization on high-mobility chemical vapor deposition grown graphene. ACS Nano, 2013, 7 (8): 7262–7270
119. Kim Y, Jhon Y I, Park J, Kim C, Lee S, Jhon Y M. Plasma functionalization for cyclic transition between neutral and charged excitons in monolayer MoS_2. Scientific Reports, 2016, 6:21405
120. Sajjad M, Morell G, Feng P. Advance in novel boron nitride nanosheets to nanoelectronic device applications. ACS Applied Materials & Interfaces, 2013, 5(11): 5051–5056
121. Nipane A, Karmakar D, Kaushik N, Karande S, Lodha S. Few-layer MoS_2 *p*-type devices enabled by selective doping using low energy phosphorus implantation. ACS Nano, 2016, 10(2): 2128–2137
122. Azcatl A, Qin X, Prakash A, Zhang C, Cheng L, Wang Q, Lu N, Kim M J, Kim J, Cho K, et al. Covalent nitrogen doping and compressive strain in MoS_2 by remote N_2 plasma exposure. Nano Letters, 2016, 16(9): 5437–5443
123. Stampfer C, Schurtenberger E, Molitor F, Guttinger J, Ihn T, Ensslin K. Tunable graphene single electron transistor. Nano Letters, 2008, 8(8): 2378–2383
124. Wang H, Maiyalagan T, Wang X. Review on recent progress in nitrogen-doped graphene: Synthesis, characterization, and its potential applications. ACS Catalysis, 2012, 2(5): 781–794
125. Jeong H M, Lee J W, Shin W H, Choi Y J, Shin H J, Kang J K, Choi J W. Nitrogen-doped graphene for high-performance ultracapacitors and the importance of nitrogen-doped sites at basal planes. Nano Letters, 2011, 11(6): 2472–2477
126. Zhang W, Lin C T, Liu K K, Tite T, Su C Y, Chang C H, Li L J. Opening an electrical band gap of bilayer graphene with molecular doping. ACS Nano, 2011, 5(9): 7517–7524
127. Nourbakhsh A, Cantoro M, Vosch T, Pourtois G, Clemente F, van der Veen M H, Hofkens J, Heyns M M, De Gendt S, Sels B F. Bandgap opening in oxygen plasma-treated graphene. Nanotechnology, 2010, 21(43): 435203
128. Ionescu R, Espinosa E H, Sotter E, Llobet E, Vilanova X, Correig X, Felten A, Bittencourt C, Van Lier G, Charlier J, et al. Oxygen functionalisation of MWNT and their use as gas sensitive thick-film layers. Sensors and Actuators. B, Chemical, 2006, 113(1): 36–46
129. Chiang W H, Lin T C, Li Y S, Yang Y J, Pei Z. Toward bandgap tunable graphene oxide nanoribbons by plasma-assisted reduction and defect restoration at low temperature. RSC Advances, 2016, 6 (3): 2270–2278
130. Han Z J, Murdock A T, Seo D H, Bendavid A. Recent progress in plasma-assisted synthesis and modification of 2D materials. 2D Materials, 2018, 5(3): 032002
131. Wojtaszek M, Tombros N, Caretta A, Van Loosdrecht P H M, Van Wees B J. A road to hydrogenating graphene by a reactive ion etching plasma. Journal of Applied Physics, 2011, 110(6): 063715
132. Radisavljevic B, Radenovic A, Brivio J, Giacometti I V, Kis A. Single-layer MoS_2 transistors. Nature Nanotechnology, 2011, 6(3): 147–150
133. Zhou W, Zou X, Najmaei S, Liu Z, Shi Y, Kong J, Lou J, Ajayan P M, Yakobson B I, Idrobo J C. Intrinsic structural defects in monolayer molybdenum disulfide. Nano Letters, 2013, 13(6): 2615–2622
134. Su J, Li N, Zhang Y, Feng L, Liu Z. Role of vacancies in tuning the electronic properties of Au-MoS_2 contact. AIP Advances, 2015, 5 (7): 077182
135. Liu D, Guo Y, Fang L, Robertson J. Sulfur vacancies in monolayer MoS_2 and its electrical contacts. Applied Physics Letters, 2013, 103(18): 183113
136. Qiu H, Xu T, Wang Z, Ren W, Nan H, Ni Z, Chen Q, Yuan S, Miao F, Song F, et al. Hopping transport through defect-induced localized states in molybdenum disulphide. Nature Communications, 2013, 4: 2642
137. Hong J, Hu Z, Probert M, Li K, Lv D, Yang X, Gu L, Mao N, Feng Q, Xie L, et al. Exploring atomic defects in molybdenum disulphide monolayers. Nature Communications, 2015, 6: 6293
138. Islam M R, Kang N, Bhanu U, Paudel H P, Erementchouk M, Tetard L, Leuenberger M N, Khondaker S I. Tuning the electrical property via defect engineering of single layer MoS_2 by oxygen plasma. Nanoscale, 2014, 6(17): 10033–10039
139. Zhang L, Zhou Y, Guo L, Zhao W, Barnes A, Zhang H T, Craig E, Zheng Y, Brahlek M, Haneef H F, et al. Correlated metals as transparent conductors. Nature Materials, 2016, 15(2): 204–210
140. Castellanos-Gomez A, Wojtaszek M, Tombros N, van Wees B J. Reversible hydrogenation and bandgap opening of graphene and graphite surfaces probed by scanning tunneling spectroscopy. Small, 2012, 8(10): 1607–1613
141. Zheng X H, Wang X L, Abtew T A, Zeng Z. Building half-metallicity in graphene nanoribbons by direct control over edge states occupation. Journal of Physical Chemistry C, 2010, 114(9): 4190–4193
142. Endo M, Hayashi T, Hong S H, Enoki T, Dresselhaus M S. Scanning tunneling microscope study of boron-doped highly

oriented pyrolytic graphite. Journal of Applied Physics, 2001, 90 (11): 5670–5674

143. Neto A C, Guinea F, Peres N M, Novoselov K S, Geim A K. The electronic properties of graphene. Reviews of Modern Physics, 2009, 81(1): 109–162
144. Kane C L, Mele E J. Quantum spin Hall effect in graphene. Physical Review Letters, 2005, 95(22): 226801
145. Young A F, Sanchez-Yamagishi J D, Hunt B, Choi S H, Watanabe K, Taniguchi T, Ashoori R C, Jarillo-Herrero P. Tunable symmetry breaking and helical edge transport in a graphene quantum spin Hall state. Nature, 2014, 505(7484): 528–532
146. Saffarzadeh A, Farghadan R. A spin-filter device based on armchair graphene nanoribbons. Applied Physics Letters, 2011, 98(2): 023106